7

Molecular Imaging of Hepatobiliary Cancers

Karthikeyan Subramanian[1] • Piyush Aggarwal[1] • Lance T. Hall[2] • Harmandeep Singh[1] • Amol M. Takalkar[2] • Bhagwant Rai Mittal[1]

[1]Department of Nuclear Medicine, Post Graduate Institute of Medical Education and Research (PGIMER), Chandigarh, India; [2]Department of Radiology and Imaging Sciences, Emory University, Atlanta, GA, USA

Author for correspondence: Bhagwant Rai Mittal, Department of Nuclear Medicine, Post Graduate Institute of Medical Education and Research (PGIMER), Chandigarh, India. Email: brmittal@yahoo.com

Cite this chapter as: Subramanian K, Aggarwal P, Hall LT, Singh H, Takalkar AM, Mittal BR. Molecular Imaging of Hepatobiliary Cancers. In: Hall LT. editor. *Molecular Imaging and Therapy*. Brisbane (AU): Exon Publications. Online first 16 Aug 2023.

Doi: https://doi.org/10.36255/molecular-imaging-of-hepatobiliary-cancers

Abstract: Currently, molecular imaging modalities are not recommended in the initial workup of hepatobiliary malignancies except in equivocal cases on conventional imaging. But the role of molecular imaging in hepatobiliary tumors is evolving and the development of new technology and molecular imaging agents has renewed the interest in molecular imaging applications in hepatobiliary malignancies. In addition to providing information for tumor staging, treatment planning, response assessment, and detection of disease recurrence, molecular imaging provides additional information on the biological and molecular behavior of the tumor to assess disease prognosis and outcome. Recent meta-analysis shows promising results favoring molecular imaging over structural imaging in hepatobiliary malignancies. Molecular imaging agents targeting different metabolic pathways (glucose and lipid metabolism) and receptors (somatostatin and fibroblast activation protein inhibitors) have been tried in hepatocellular carcinoma, cholangiocarcinoma, liver metastasis and neuroendocrine tumors. We explore and summarize the current role of molecular imaging in hepatobiliary tumors and its

In: Hall LT. editor. *Molecular Imaging and Therapy*. Brisbane (AU): Exon Publications. ISBN: 978-0-6458663-9-1. Doi: https://doi.org/10.36255/molecular-imaging

advantages and disadvantages over conventional imaging modalities, along with a brief overview of newer PET molecular imaging agents.

Keywords: cholangiocarcinoma; hepatocellular carcinoma; molecular imaging; neuroendocrine tumor; positron emission tomography

INTRODUCTION

Malignancies of the liver can be either primary or secondary metastases. The most common primary liver cancer is hepatocellular carcinoma (HCC). Worldwide, HCC is the fourth most common cause of cancer-related death and is detected in over 800,000 new cases each year (1). HCC frequently affects people with chronic liver disease secondary to hepatitis or alcoholic cirrhosis. Secondary metastases to the liver commonly occur from colorectal cancer and neuroendocrine tumors.

^{18}F-FDG PET IN HEPATOCELLULAR CARCINOMA

The most common currently employed nuclear molecular imaging method for detecting liver tumors is fluorine-18 fluorodeoxyglucose positron emission tomography (^{18}F-FDG PET), which has demonstrated efficacy in predicting prognosis, staging, response assessment, and recurrence detection (2).

Staging of HCC

The prognosis of HCC is influenced by the disease stage at the time of presentation. Patients with larger tumors and metastatic disease have worse prognoses. While locally advanced HCC without extrahepatic dissemination may be treated with intensive local therapy, HCC with extrahepatic metastases has a poor prognosis and limited treatment options. Triple phase computed tomography (TPCT) and contrast enhanced magnetic resonance imaging (ceMRI) are modalities of choice for detection of HCC, targeting the increased blood supply to HCC via hepatic artery. Histopathological sampling is not needed in establishing the diagnosis of HCC if characteristic findings are present on TPCT or ceMRI.

Detection of primary HCC using ^{18}F-FDG PET/CT alone is limited, with a relatively low sensitivity (approx. 50–65%) compared to current standard of care imaging. Higher grades of HCC (less differentiated) tend to have higher FDG avidity, whereas well-differentiated HCC shows relatively low ^{18}F-FDG uptake (3). This results from the varied expression of glucose transporters (GLUT) and increased glucose-6-phosphatase activity in well differentiated HCC while poorly differentiated HCC has loss of glucose-6-phosphatase activity. In a study by Torizuka et al., the degree of differentiation of HCC was correlated with ^{18}F-FDG uptake, with higher-grade tumors showing twice FDG uptake compared to lower-grade tumors (4). Dual point imaging can be performed, in addition to the conventional imaging 1-hour after FDG injection, to increase the sensitivity of ^{18}F-FDG PET/CT to detect HCC (5). Figure 1 shows ^{18}F-FDG PET/CT findings in primary HCC.

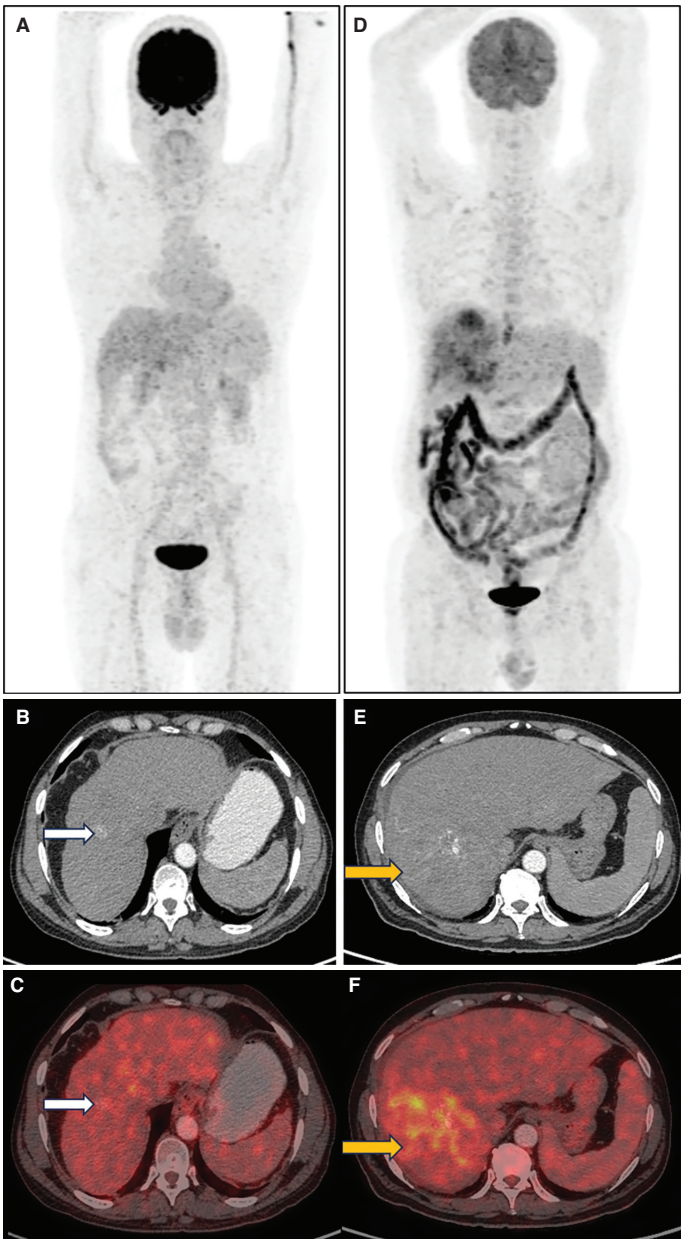

Figure 1. ^{18}F-FDG PET/CT in HCC. A. Maximum Intensity Projection (MIP) image of ^{18}F-FDG PET/CT in a patient with well-differentiated HCC shows no abnormal increased tracer uptake in the liver. Corresponding CT **(B)** and fused PET/CT **(C)** images for the same patient show non-FDG avid arterially enhancing lesion in segment VIII of liver, consistent with primary HCC (white arrows). **D.** Maximum Intensity Projection (MIP) image of ^{18}F-FDG PET/CT in a patient with poorly differentiated HCC showing areas of increased FDG uptake in the liver. Corresponding CT **(E)** and fused PET/CT **(F)** images in the second patient show FDG avid (SUVmax 9.4) arterially enhancing mass involving the segments VI and VII of liver (yellow arrows).

HCC commonly metastasizes to regional lymph nodes, lungs, bone, and rarely to peritoneum and other organs. ^{18}F-FDG PET/CT has demonstrated good efficacy in diagnosing distant metastases from HCC. It outperforms conventional imaging modalities to detect bone involvement while demonstrating equal detection rates for lung and nodal disease. Various studies have shown that ^{18}F-FDG PET-CT has sensitivity and specificity around 77% and 98%, respectively for extrahepatic metastases (6–8).

The much higher sensitivity of ^{18}F-FDG PET for detecting distant metastases in HCC compared to primary HCC may be due to the higher incidence of metastases in poorly differentiated HCC, which tends to have more ^{18}F-FDG uptake. Compared to multidetector computed tomography (MDCT) and bone scintigraphy, ^{18}F-FDG PET/CT has a better sensitivity for bone metastases.

Portal vein tumor thrombus (PVTT) also demonstrates high ^{18}F-FDG avidity. Imaging findings of PVTT in HCC include contrast enhancement, intraluminal filling defect, and ^{18}F-FDG avidity in the thrombus (9). Vascular invasion in patients with HCC before liver transplant is one of the major reasons for HCC recurrence after transplantation. ^{18}F-FDG PET/CT before liver transplant has a good predictive value for vascular invasion in patients with HCC which is helpful in determining the prognosis and selecting the suitable candidates for liver transplantation in HCC. Higher intensity of FDG uptake can be a potential indicator of vascular invasion. In a study by Lin et al., patients with vascular invasion had higher T_{SUVmax} (tumor SUVmax) and T_{SUVmax}/L_{SUVmax} ratio (ratio of tumor SUVmax to normal liver SUVmax) compared to patients without vascular invasion (10).

Response assessment

Surgical resection and locoregional therapies such as trans-arterial chemoembolization (TACE), radiofrequency ablation (RFA) and trans-arterial radioembolisation (TARE) using ^{90}Y/radio-labelled microspheres can be used to treat early-stage HCC. In unresectable, non-metastatic HCC, liver transplantation is an alternate treatment option. Before a liver transplant, patients can be downstaged with locoregional treatments (LRT). Hence, determining the tumor's response to LRT is crucial in managing HCC. Locally targeted therapy (LRT) for HCC causes tumor cell death through ischemia by reducing blood flow to the tumor and by radiation effects. This does not cause the tumor to shrink but causes necrosis and a reduction in the enhancement pattern.

Functional imaging techniques like PET/CT and diffusion-weighted magnetic resonance imaging (DW MRI) help evaluate HCC patients after treatment intervention. In their study, Nashi et al. compared ^{18}F-FDG PET/CT to DW MRI and found DW MRI was more accurate at detecting residual and recurrent hepatic tumors due to the addition of a quantitative assessment using the ADC value (11). To ascertain residual tumors, ^{18}F-FDG PET/CT showed greater sensitivity than conventional imaging techniques such as contrast-enhanced computed tomography (CECT), often characterized by a focused eccentric uptake in the periphery. According to studies, patients who exhibit a considerable reduction in SUVmax or SUV ratio (ratio of tumor SUVmax to liver background SUVmax) after treatment have improved survival and event-free rates (12, 13). Low ^{18}F-FDG uptake has been found to be associated with prolonged progression-free survival (PFS) and

overall survival (OS) in HCC patients receiving chemoradiation therapy. Conversely, high ^{18}F-FDG uptake was associated with a higher risk of extrahepatic metastasis within six months (14).

Recurrence evaluation

The long-term prognosis for patients with HCC is poor as HCC has a high recurrence rate, ranging from 51–90% after surgical resection. Early detection of recurrent HCC is greatly aided by rising serum alpha-fetoprotein (AFP) or protein induced vitamin K absence or antagonist II (PIVKA II) measurements, ultrasound, and CT of the abdomen. Few studies have evaluated the usefulness of ^{18}F-FDG PET/CT in recurrent HCC. A systematic review and metanalysis by Lin et al. showed that the sensitivity and specificity of ^{18}F-FDG PET/CT in the detection of recurrent HCC were 81.7% (95% CI: 71.6–89.4%) and 88.9% (95% CI: 70.8–97.6%) respectively (15).

Pre and post TARE imaging in HCC

^{99m}Tc-macro-aggregated albumin (MAA) scintigraphy is performed during planning for TARE in HCC to determine targeted ^{90}Y-microsphere delivery to the lesion and shunting to lungs and other organs. Post therapy imaging can be done in patients undergoing ^{90}Y-microsphere trans-arterial radioembolization by bremsstrahlung imaging utilizing the SPECT/CT scanner or by PET/CT examination using positrons emitted by internal pair production from ^{90}Y. Utility of post TARE imaging includes demonstrating whether the spheres have localized at the targeted tumor site as planned, and detecting abnormal ^{90}Y-microsphere localization to the stomach or elsewhere, which can lead to adverse effects such as ulceration. The post-treatment scan also enables the determination of the dose supplied to the tumor, which is a predictor of tumor response.

OTHER PET MOLECULAR IMAGING AGENTS IN HCC

Due to the limitations of ^{18}F-FDG PET in well-differentiated HCCs, many radiopharmaceuticals targeting other metabolic pathways or receptors have been developed and evaluated in HCC.

^{68}Ga-or ^{18}F-PSMA PET

PSMA (prostate specific membrane antigen), a type II transmembrane protein is typically expressed in prostate tissue. PSMA can be overexpressed in pathophysiological processes other than prostate cancer, such as the neovasculature of numerous malignant tumours including HCC. This allows the use of PSMA ligand-based PET/CT in the evaluation of HCC. In HCC staging, the accuracy of PSMA PET/CT is comparable to that of CT for intrahepatic disease detection and more accurate than CT for extrahepatic disease detection. Due to is higher accuracy in detecting extrahepatic disease, PSMA PET/CT is valuable for early identification of patients for systemic therapy (16). PSMA PET/CT also has theranostic potential to select patients showing PSMA uptake for treatment with therapeutic radionuclides.

^{11}C-acetate PET

^{11}C-acetate is one such molecular imaging agent that has been used to overcome the low uptake and retention of ^{18}F-FDG in well-differentiated HCCs. Acetate is taken up by HCC cells and transformed into acetyl-CoA by acetyl-CoA synthetase. Participation in free fatty acid (lipid) synthesis is thought to be the most common mechanism of incorporation of radiolabeled acetate in tumors. Fatty acids and cholesterol that have been ^{11}C-labelled are quickly absorbed into the cell membranes by tumor cells that overexpress fatty acid synthetase or acetyl-CoA carboxylase, permitting the use of ^{11}C-acetate PET/CT for tumor detection. Thirty-nine HCC patients were included in a PET/CT study by Ho et al. comparing uptake of ^{11}C-acetate and ^{18}F-FDG uptake in HCC lesions. They determined poorly differentiated lesions predominantly accumulate ^{18}F-FDG, whereas well-differentiated lesions predominantly accumulate ^{11}C-acetate (17). Park et al. concluded that ^{11}C-acetate PET was more sensitive than ^{18}F-FDG PET (75.4% vs. 60.9%) in detecting HCC (18). ^{11}C is a cyclotron produced radionuclide with a half-life of 20 minutes. This short half-life makes the commercial availability of ^{11}C based PET tracers difficult as a closely located cyclotron facility is necessary for widespread adoption.

^{68}Ga-FAPI PET

Fibroblasts associated with malignancy are known to be involved in tumor growth, migration, and progression. Fibroblast activation protein (FAP) is a serine protease highly expressed in cancer associated fibroblasts (CAF). As CAFs make about 90% of the gross tumor mass, targeting FAP inhibitor (FAPI) for imaging can aid in the visualisation of the tumor stroma. Guo et al. compared CECT, liver MRI, ^{68}Ga-FAPI and ^{18}F-FDG PET/CT in diagnosing primary and metastatic lesions in patients with HCC. Thirty-four individuals with hepatic lesions were included in the study and underwent concomitant ^{68}Ga-FAPI-04, ^{18}F-FDG PET, and CT scans. In the detection of primary liver tumors, the sensitivities of CECT, MRI, ^{68}Ga-FAPI-04, and ^{18}F-FDG PET/CT were found to be 96%, 100%, 96%, and 65%, respectively (19). ^{68}Ga-FAPI PET/CT also has the potential to open the door for theranostic treatment option with therapeutic radionuclides in select patients showing ^{68}Ga-FAPI uptake. Figure 2 (A-D) shows comparison of ^{18}F-FDG and ^{68}Ga-FAPI PET in a case of HCC.

^{18}F-Fluorocholine PET

The cell membrane consists of phospholipids in which choline is one of the essential components. Compared to normal liver tissue, HCC cells have a large amount of choline. The ability of tumor cells to integrate choline actively to form phosphatidylcholine, a component of the cell membrane, and promote quick cell division, is what distinguishes them from normal cells. When ^{18}F-fluorocholine enters the tumor cell, it is quickly phosphorylated to ^{18}F-phosphorylcholine and trapped within the cell membranes. In a prospective study, the ability of ^{18}F-fluorocholine and ^{18}F-FDG to detect and stage HCC in patients with chronic liver disease and suspicious hepatic nodules was evaluated. According to this study, ^{18}F-fluorocholine was significantly more sensitive than ^{18}F-FDG (94 vs. 59%) in detecting HCC, particularly in well-differentiated tumors (20).

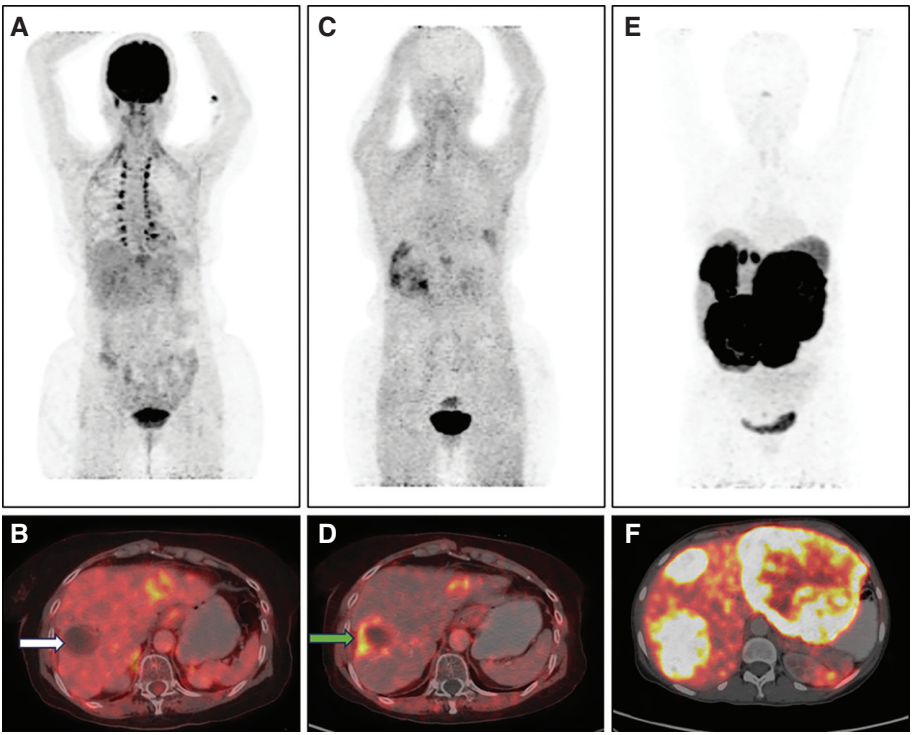

Figure 2. ^{18}F-FDG, ^{68}Ga-FAPI PET/CT in HCC and ^{68}Ga-DOTANOC PET/CT in NET. A. Maximum Intensity Projection (MIP) image of ^{18}F-FDG PET/CT showing increased tracer uptake in the left lobe of liver in a case of HCC. Corresponding fused ^{18}F-FDG PET/CT **(B)** image shows a non-FDG avid lesion in segment VII of liver (white arrow) and FDG avid lesion in left lobe. **C.** MIP image of ^{68}Ga-FAPI PET/CT in the same patient showing areas of increased FAPI uptake in both lobes of the liver with corresponding fused transaxial ^{68}Ga-FAPI PET/CT **(D)** image showing FAPI avidity (SUVmax 9.8) in the same segment VII and left lobe liver lesions (green arrow). ^{68}Ga-FAPI PET can detect more lesions with higher tracer uptake compared to ^{18}F-FDG PET-CT in HCC. **E.** MIP image of ^{68}Ga-DOTANOC PET/CT in another patient with neuroendocrine tumor showing intense tracer uptake in the liver in multiple areas. Corresponding fused axial PET/CT image **(F)** shows intensely somatostatin receptor expressing lesions in both lobes of the liver, consistent with metastatic NET. ^{68}Ga- DOTANOC PET/CT is highly specific for neural crest origin tumors.

Neuroendocrine tumors of the liver

Neuroendocrine neoplasms are relatively less common tumors and can arise from neuroendocrine cells present anywhere in the body. Neuroendocrine tumors (NETs) frequently originate from the gastrointestinal tract, adrenal glands, and lungs, and they metastasize commonly to the liver and bone. NETs of the liver can either be primary (rare) or metastatic (common).

Molecular imaging methods useful in diagnosis, staging and metastasis evaluation of NETs include ^{111}In-pentetreotide somatostatin receptor scintigraphy (^{111}In-SRS), ^{68}Ga-DOTATATE, ^{68}Ga-DOTANOC, and ^{18}F-DOPA PET/CT for well-differentiated tumors and ^{18}F-FDG PET/CT for high grade tumors. Somatostatin receptor (SSTR) overexpression is present in 60–90% of these tumors and is an

essential mechanism for SRS. Of these, somatostatin receptor subtype 2 is expressed by 85% of NETs. Recent experience with ^{68}Ga-labeled somatostatin analogue PET imaging shows higher sensitivity as compared to ^{111}In-SRS and ^{99m}Tc-SRS. ^{111}In-SRS and ^{99m}Tc-SRS are used less due to lower sensitivity and resolution compared to ^{68}Ga-DOTA-NOC/TATE PET/CT. The diagnostic efficacy of ^{68}Ga-DOTATATE PET/CT was compared to that of ^{99m}Tc-octreotide SPECT/CT and CT/MRI by Fallahi et al. In this prospective study, 25 NET patients who had been referred for an octreotide scan for suspected or proven NET were included. On a patient-based analysis, the sensitivity for CT/MRI, ^{68}Ga-DOTATATE PET/CT, and ^{99m}Tc-octreotide SPECT/CT, respectively, was 71%, 90%, and 65%. The specificity of ^{99m}Tc-octreotide SPECT/CT, ^{68}Ga-DOTATATE PET/CT, and CT/MRI was 80%, 80%, and 75%, respectively (21). Figure 2 (E-F) shows ^{68}Ga-DOTANOC PET/CT images in a case of metastatic well-differentiated NET.

As primary hepatic NET (PHNET) is uncommon, only after a primary extrahepatic source has been ruled out can the presence of PHNET be confirmed. The staging and prognosis of PHNETs are not thoroughly understood. The most effective treatment for PHNET is surgical resection. Liver is one of the common sites for metastatic NET and is an important adverse prognostic predictor in enteropancreatic NET patients, occurring in 65–95% of cases.

High-grade (G3) and poorly differentiated NETs have low expression of SSTRs, but high metabolic activity. Therefore, ^{18}F-FDG PET/CT is preferred in evaluating poorly differentiated NET tumors as it does not rely on the presence of SSTRs for uptake. To summarise, ^{68}Ga-SRS should be considered for molecular imaging of well-differentiated NETs with a low Ki67 as these tumors will more likely have a higher density of SSTRs compared with poorly differentiated tumors with higher Ki67 values. When assessing tumors with a high Ki67, ^{18}F-FDG PET/CT should be considered. Finally, these imaging technologies have greatly enhanced the utility of molecular imaging in NETs in comparison to CT or MRI. ^{18}F-DOPA, ^{11}C-5-hydroxy-tryptophan and ^{64}Cu-DOTATATE are other radiopharmaceuticals that can be useful in molecular imaging of liver NET.

^{64}Cu-DOTATATE PET/CT imaging has few added advantages over ^{68}Ga-SRS. ^{64}Cu has a longer half-life ($t_{1/2}$ of 12.7 hours) due to which it has a higher shelf life of more than 24 hours and scanning window of more than 3 hours allowing flexibility in patient scheduling. ^{64}Cu is cyclotron-produced radionuclide, hence it eliminates the requirement of in-house generator. In a study by Johnbeck et al., head-to-head comparison of ^{64}Cu-DOTATATE and ^{68}Ga-DOTANOC PET/CT revealed that ^{64}Cu-DOTATATE showed 42 lesions not found on ^{68}Ga-DOTATOC, of which 33 were found to be true-positive on follow-up (22).

Patients with metastatic, inoperable, well-differentiated NETs who exhibit tumor uptake higher than liver in SRS imaging are candidates for Peptide Receptor Radionuclide Therapy (PRRT). ^{64}Cu-DOTATATE and ^{68}Ga-DOTANOC PET/CT imaging has a vital role in patient selection for radionuclide therapies in NET patients.

HEPATIC METASTASES

Metastases to the liver occur more frequently than primary liver tumors. The primary malignancies of the GI tract, breast, lung, pancreatic, and sarcomas are

common sources of metastatic lesions in the liver. Detecting hepatic metastases during tumor staging is crucial as it alters the treatment strategy.

Detection of hepatic metastases during initial staging in malignancy

In a few studies, contrast enhanced MRI (CEMRI) has shown superior results compared to CECT and ^{18}F-FDG PET/CT for detecting liver metastases, especially for smaller lesions. However, ^{18}F-FDG PET/CT is frequently employed in evaluating many malignancies since it can simultaneously identify hepatic metastases as well as extrahepatic lesions.

The tumor's differentiation or histopathologic characteristics fundamentally determine the extent of ^{18}F-FDG uptake. Metastases typically exhibit a biological character comparable to the primary tumor though can be more poorly differentiated compared to the primary tumor in some cases due to selection of aggressive phenotypes. Most liver metastases have increased ^{18}F-FDG uptake, which correlates with the increased expression of GLUT-1 in primary tumors of the colorectum, pancreas, breast, and lung.

Some of the tumors with decreased glucose metabolism include bronchioloalveolar carcinoma of the lung, prostate cancer, and low-grade neuroendocrine tumors. As with the primary tumor, liver metastases from these tumors can have low ^{18}F-FDG uptake. Similarly, since the number of viable cancer cells or metabolically active tumor volume impacts visualization of ^{18}F-FDG uptake, mucinous tumors may not demonstrate high ^{18}F-FDG uptake. Hence, hepatic metastases from the mucinous GI tract or mucinous ovarian tumors may not show high ^{18}F-FDG uptake.

Assessing the response of hepatic metastases to therapies

Evidence supports using ^{18}F-FDG PET/CT in evaluating tumor response to treatment. Interestingly, overall survival has been shown to be predicted by SUV from ^{18}F-FDG PET/CT before treatment, but not by SUV after treatment, according to a meta-analysis by Xia et al. (23). The post treatment SUV values are not reliable for predicting overall survival because the post treatment inflammatory changes may also show FDG uptake. ^{18}F-FDG PET/CT can provide the extra benefit of being able to identify a tumor's metabolic response when compared to anatomical cross-sectional imaging. Some studies have shown no additional benefit of ^{18}F-FDG PET over CT or MRI in evaluating liver lesions post-treatment, as neoadjuvant therapy may decrease the sensitivity of ^{18}F-FDG PET. In a study by Lubezky et al., it was concluded that the sensitivity of ^{18}F-FDG PET in detecting hepatic metastasis after neoadjuvant chemotherapy is lower as compared to the CECT (49 vs. 65%) (24).

PET/MRI in HCC

Oncologic imaging is one of the main potential uses for hybrid positron emission tomography/magnetic resonance imaging (PET/MRI), which is becoming more widely available. The soft tissue contrast provided by MRI is used as anatomical references for PET measurements. Functional MRI approaches can also support

PET-based tumor characterisation. Only few studies are available regarding the utility of hybrid PET/MRI in HCC. One such study showed a negative correlation between FDG-PET SUV and apparent diffusion coefficient in MRI (25). Further studies with large sample size are required to explore the role of hybrid PET/MRI in HCC.

Radiomics in HCC

Radiomics is an evolving field that uses high-dimensional medical imaging to extract quantitative data that can be mined but cannot be seen with the human eye. Radiomic models in HCC can be used to predict histology (differentiating benign and malignant tumours, prediction of histologic grade and microvascular invasion), HCC genetic expression (Ki-67, CK-19 and p53), treatment response, recurrence, survival and assessing immune status (PD-L1) of the tumour to select patient for immunotherapy.

BILIARY TRACT CANCERS (BTCs)

BTCs can arise from the gall bladder (GB cancer) or the biliary ducts (cholangiocarcinoma). Cholangiocarcinoma (CCA) is further classified as intrahepatic (iCCA) and extrahepatic (eCCA) types. The former arises from the biliary tree proximal to segmental bile ducts, while the latter can be subdivided into perihilar (right and left hepatic ducts or their junction) and distal CCA (distal to cystic duct insertion) (26, 27).

Gallbladder carcinoma (GBC)

Histopathological sampling using cytology or biopsy is the gold standard investigation for diagnosing GBC. However, imaging modalities have a crucial role, especially in patients with repeated negative findings or inadequate sampling, owing to challenges in lesion accessibility (28). Staging the disease is the first step in the management of BTCs. Owing to its superior soft tissue resolution, magnetic resonance cholangiopancreaticography (MRCP) is the imaging modality of choice for tumor (T) staging, while CECT is recommended for nodal (N) and metastatic (M) staging (29, 30).

The role of ^{18}F-FDG PET/ CT in the management of GBC is still evolving and there is increasing evidence supporting its critical role in staging and restaging of GBC. A recent meta-analysis by Lamarca et. al. reported a pooled sensitivity of 88.4% (95% CI 82.6–92.8) and specificity of 72.3% (95% CI 60.7–82.1) for ^{18}F-FDG PET in the diagnosis of primary GBC 28). The primary lesion usually presents as a luminal mass, polypoidal lesion or asymmetrical mural thickening (31). Many benign and malignant lesions with high ^{18}F-FDG uptake can mimic gallbladder carcinoma resulting in lower specificity. Benign lesions such as acute cholecystitis or xanthogranulomatous cholecysitits, tuberculosis, adenomyomatosis, IgG4 related disease or malignant lesions like hepatocellular carcinoma, cholangiocarcinoma and metastatic lesions infiltrating the gallbladder fossa can mimic GBC (false positive) and complicate the scan interpretation (32–34). On the other hand, smaller lesions (<1 cm) and mucinous variants tend to show low ^{18}F-FDG uptake resulting in relatively lower sensitivity.

Many studies have tried to define standardized uptake values (SUV) for differentiating benign from malignant lesions, with benign lesions showing a lower mean SUVmax (1.8) than malignant lesions (8.53) (28). However, these results are not universally applicable, and many variations and exceptions exist. Dual time point imaging can help to differentiate between benign and malignant lesions with malignant lesions showing increased uptake and tumor to background ratio on delayed ^{18}F-FDG PET images compared to early images (35).

Although the pooled sensitivity of ^{18}F-FDG PET/CT is high for lymph nodal spread in GBC [93.8 (95% CI 82.8–98.7)], false negative scans due to micrometastatic lymph node disease or mucinous variant of GBC are not uncommon (28). However, pooled specificity for lymph node disease is lower [70.4 (49.8–86.2)] due to false positive uptake in granulomatous inflammation, reactive nodes and other abdominal infections which are difficult to distinguish from metastases without pathological confirmation (28). The pooled sensitivity for distant metastasis is 91.1% (95% CI 82.6–96.4) with false negative findings in metastases from mucinous variant, micrometastatic peritoneal and liver nodules, while pooled specificity is 82.4% (95% CI 71.8–90.3) with false positive findings in patients with liver or cholangitic abscesses and granulomatous inflammation (sarcoidosis, IgG4 related disease, etc) (28, 36, 37).

^{18}F-FDG PET also proved to be superior to conventional imaging in detecting relapse in GBC with a pooled sensitivity of 93.6% (95% CI 82.5–98.7) and pooled specificity of 90.9% (95% CI 70.8–98.9) (28, 38). Overall, ^{18}F-FDG PET/CT upstaged the disease and changed the management in around 15% patients in a study (28). Moreover, high SUV uptake in lesions at baseline (signifying poorly differentiated pathology or other aggressive variants) has a prognostic significance resulting in a worse progression-free survival and overall survival [28, 39, 40]. Similarly, outcome is better if there is a significant reduction in the lesion SUVmax after chemotherapy (39, 40).

Current guidelines do not recommend ^{18}F-FDG PET/CT for primary diagnosis of GBC, but acknowledge its role in detecting nodal and distant metastases, and disease recurrence, especially in equivocal cases on conventional imaging (29, 41). Compared to ^{18}F-FDG PET/CT, preliminary results using ^{68}Ga-FAPI PET/CT have shown higher sensitivity and specificity for primary and metastatic GBC with higher ^{68}Ga-FAPI uptake in neoplastic lesions and a significantly lower average SUVmax in inflammatory lesions (42). Results of ongoing studies can validate the usefulness of FAPI PET in GBC.

Cholangiocarcinoma

Similar to GBC, MRI remains the imaging modality of choice for the accurate diagnosis, staging and assessing resectability in intrahepatic and extrahepatic cholangiocarcinoma. CECT of the chest, abdomen and pelvis is recommended to evaluate for distant spread of disease (41). The role of ^{18}F-FDG PET in CCA is continuously evolving as more multicenter prospective studies are being conducted. The pooled sensitivity of ^{18}F-FDG PET/CT for detection of a primary lesion in CCA is more than 90%, however the pooled specificity is lower, especially for eCCA, ranging from 20–35% (28). This is due to a high incidence of false positive ^{18}F-FDG uptake in primary sclerosing cholangitis (PSC), acute cholangitis, biliary prosthesis/stent site, benign stricture, biliary adenoma, granulomatous

inflammation and infection-related false-positive findings (29, 43). ^{18}F-FDG PET/CT should ideally be scheduled before any biliary intervention to avoid any inflammatory stent-related ^{18}F-FDG uptake.

Histologically, the majority of perihilar and distal CCA are mucinous adenocarcinomas or papillary tumors (44). Mucin itself does not take up ^{18}F-FDG, thus the scant tumor cells present may be insufficient to produce a detectable PET signal, especially amidst the surrounding high background liver activity. Additionally, these tumors often exhibit desmoplastic stroma reaction, where the tumor cells are loosely dispersed within connective tissue, providing insignificant volume for PET detection in many cases (45).

Extrahepatic CCAs present as infiltrative, exophytic or polypoidal lesions (46). The most common infiltrative subtype requires careful evaluation and is difficult to detect using CECT and ^{18}F-FDG PET. Other pathologies such as cholangitis also present with enhancing biliary duct thickening and can be easily misinterpreted. ^{18}F-FDG PET detection of small and narrow lesions may be obscured by the partial volume effect, respiratory movement-related artefacts and the high surrounding liver and intestinal activity (47).

For lymph node and distant metastatic spread, pooled sensitivity (55.6% and 72.7% respectively) and specificity (63% and 77.5% respectively) of ^{18}F-FDG PET/CT were shown to be moderate in CCA, especially for perihilar CCA (28). Dual time point imaging has been shown to be superior to early PET images in detecting regional lymph nodal metastasis, with a higher sensitivity, specificity, positive and negative predictive value and diagnostic accuracy (47). Dual time point imaging was not useful for distant metastatic sites. Nonetheless, the diagnostic accuracy of ^{18}F-FDG PET for the detection of lymph node and distant metastases is higher compared to CT and it provides additional information for equivocal lesions on conventional imaging (42, 46).

Intrahepatic CCA presents as mass forming, periductal infiltrating or intraductal growth (26). Unlike eCCA, ^{18}F-FDG PET/CT has a higher diagnostic accuracy for detection of primary and distant spread of disease in iCCA (28). This may be attributed to different tumor metabolic characteristics in lymph node and distant metastatic sites as compared to eCCA (48). Due to its high sensitivity for detection of regional and distant metastatic disease spread, it can be helpful in avoiding unnecessary surgery, though pathological confirmation is still required for upstaging the disease. In those with locally advanced disease, it helps direct the extent of surgical resection and localizes the regional lymph nodes, which may require histopathological sampling. However, ^{18}F-FDG PET has some limitations in iCCA, similar to eCCA.

Various PET quantitative parameters such as SUV, metabolic tumor volume (MTV) and tumor lesion glycolysis (TLG) accurately detect the baseline tumor bulk and total body disease burden and have a significant role in disease prognosis and management (48). The primary tumor SUVmax is an independent prognostic factor for survival outcomes in CCA and for predicting metastases on follow-up (48). Calculating volumetric parameters is tedious and time consuming, however technological advances in the form of automated volumetric analysis and threshold-based segmentation have made it more convenient. Newer acquisition techniques like dynamic ^{18}F-FDG PET imaging have shown to be superior to conventional imaging in detecting and excluding CCA in advanced PSC with lesion/liver ratio being significantly higher in parametric images than static

PET images (49). Not only can it help to differentiate normal from malignant tissue, kinetic modeling and analysis also helps to differentiate hepatocellular cancer from CCA (50). Figure 3 shows ^{18}F-FDG PET-CT findings in common BTCs.

^{68}Ga-FAPI PET overcomes some of the shortcomings of ^{18}F-FDG PET. It has a higher tumor uptake and tumor to background ratio. In addition, it can detect additional micrometastatic lesions that can be missed on ^{18}F-FDG PET, due to higher contribution of fibroblasts to the tumor volume (41,51). Additionally,

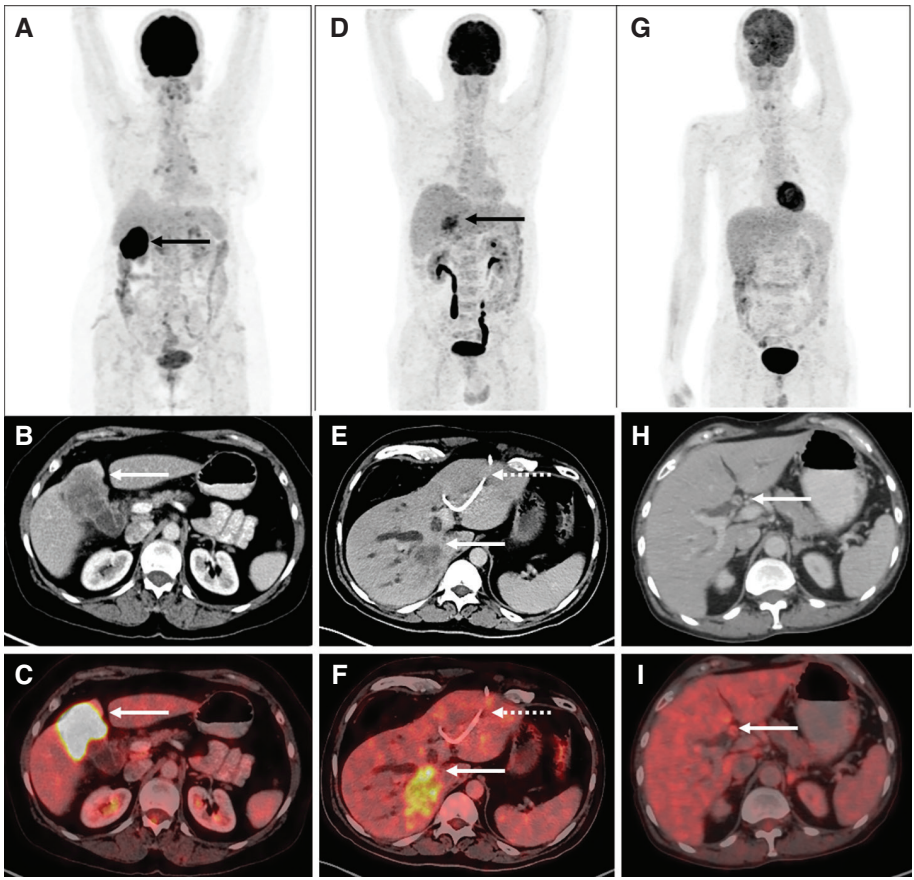

Figure 3. ^{18}F-FDG PET/CT in biliary tract cancers: A) Maximum Intensity Projection (MIP) image showing focal intense tracer uptake in the region of the gallbladder fossa (black arrow). Corresponding CT **(B)** and fused PET/CT **(C)** images show intensely tracer avid (SUVmax 28.7) heterogeneously enhancing mass lesion arising from the fundus and body of the gallbladder with local invasion (Gallbladder carcinoma) (white arrows). **D)** MIP image showing tracer uptake in the region of the liver (black arrow) with corresponding CT **(E)** and fused PET/CT **(F)** images showing ^{18}F-FDG avid (SUVmax 11.2) hypodense lesion in the right lobe of liver (white arrows) causing intrahepatic biliary radical dilatation suggestive of intrahepatic cholangiocarcinoma along with percutaneous transhepatic biliary duct stent in situ in the left ductal system (dotted arrows). **G)** MIP image with no abnormal focus of uptake seen anywhere in the region of the liver. Corresponding CT **(H)** and fused PET/CT **(I)** images show faintly tracer avid biliary ductal thickening (SUVmax 5.1) in the hilar region with tracer uptake similar to background liver uptake suggestive of hilar cholangiocarcinoma.

labeling FAPI with Lutetium-177 (^{177}Lu), Yttrium-90 (^{90}Y) or Holmium-166 (^{166}Ho), may provide new therapeutic options in patients who have progressed despite conventional treatment regimens (52). Further studies with larger sample sizes are required to conclude the role of ^{68}Ga-FAPI PET/CT in CCA.

CONCLUSION

^{18}F-FDG PET/CT and newer promising PET molecular imaging agents as well as PET/MRI have an evolving role in the imaging of hepatobiliary tumors with potential advantages over conventional imaging modalities. ^{18}F-FDG PET performs well in poorly differentiated HCC whereas ^{11}C-acetate performs better in well differentiated HCC. In intrahepatic cholangiocarcinoma, ^{18}F-FDG PET shows promising role, while ^{68}Ga-FAPI PET/CT has shown good uptake in both HCC and extrahepatic cholangiocarcinomas. Novel PET molecular imaging agents also have the promise of selecting patients for targeted radionuclide therapy.

Conflict of Interest: The authors declare that they have no potential conflict of interest with respect to the research, authorship, and/or publication of this chapter.

Copyright and Permission Statement: The authors confirm that the materials included in this chapter do not violate copyright laws. Where relevant, appropriate permissions have been obtained from the original copyright holder(s), and all original sources have been appropriately acknowledged or referenced. Where relevant, informed consent has been obtained from patients or their caregivers according to applicable national or institutional policies.

REFERENCES

1. Bray F, Ferlay J, Soerjomataram I, Siegel RL, Torre LA, Jemal A. Global cancer statistics 2018: GLOBOCAN estimates of incidence and mortality worldwide for 36 cancers in 185 countries. CA Cancer J Clin. 2018;68(6):394–424. https://doi.org/10.3322/caac.21492
2. Eo JS, Paeng JC, Lee DS. Nuclear imaging for functional evaluation and theragnosis in liver malignancy and transplantation. World J Gastroenterol. 2014;20(18):5375–88. https://doi.org/10.3748/wjg.v20.i18.5375
3. Sacks A, Peller PJ, Surasi DS, Chatburn L, Mercier G, Subramaniam RM. Value of PET/CT in the management of liver metastases, part 1. AJR Am J Roentgenol. 2011;197(2):W256–9. https://doi.org/10.2214/AJR.10.6331
4. Torizuka T, Tamaki N, Inokuma T, Magata Y, Yonekura Y, Tanaka A et al. Value of fluorine-18-FDG-PET to monitor hepatocellular carcinoma after interventional therapy. J Nucl Med. 1994;35(12):1965–9.
5. Wu B, Zhao Y, Zhang Y, Tan H, Shi H. Does dual-time-point 18F-FDG PET/CT scan add in the diagnosis of hepatocellular carcinoma? Hell J Nucl Med. 2017;20(1):79–82.
6. Sugiyama M, Sakahara H, Torizuka T, et al. 18F-FDG PET in the detection of extrahepatic metastases from hepatocellular carcinoma. J Gastroenterol 2004;39:961–8. https://doi.org/10.1007/s00535-004-1427-5
7. Ho CL, Chen S, Yeung DW, Cheng TK. Dual-tracer PET/CT imaging in evaluation of metastatic hepatocellular carcinoma. J Nucl Med. 2007;48(6):902–9. https://doi.org/10.2967/jnumed.106.036673

8. Seo HJ, Kim GM, Kim JH, Kang WJ, Choi HJ. ^{18}F-FDG PET/CT in hepatocellular carcinoma: detection of bone metastasis and prediction of prognosis. Nucl Med Commun. 2015;36(3):226–33. https://doi.org/10.1097/MNM.0000000000000246
9. Nguyen XC, Nguyen DS, Ngo VT, Maurea S. FDG-Avid Portal Vein Tumor Thrombosis from Hepatocellular Carcinoma in Contrast-Enhanced FDG PET/CT. Asia Ocean J Nucl Med Biol. 2015;3(1):10–7.
10. Lin CY, Liao CW, Chu LY, Yen KY, Jeng LB, Hsu CN, Lin CL, Kao CH. Predictive Value of 18F-FDG PET/CT for Vascular Invasion in Patients With Hepatocellular Carcinoma Before Liver Transplantation. Clin Nucl Med. 2017;42(4):e183-e187. https://doi.org/10.1097/RLU.0000000000001545
11. Nashi, I.T., Morsy, H.A., Shalaby, M. h. et al. Role of 18F-FDG PET/CT in assessment of HCC patients after therapeutic interventions compared to DW MRI. Egypt J Radiol Nucl Med 53, 186 (2022). https://doi.org/10.1186/s43055-022-00867-0
12. Lee SM, Kim HS, Lee S, Lee JW. Emerging role of 18F-fluorodeoxyglucose positron emission tomography for guiding management of hepatocellular carcinoma. World J Gastroenterol. 2019;25(11):1289–1306. https://doi.org/10.3748/wjg.v25.i11.1289
13. Han S, Choi JY. Prognostic value of 18F-FDG PET and PET/CT for assessment of treatment response to neoadjuvant chemotherapy in breast cancer: a systematic review and meta-analysis. Breast Cancer Res. 2020;22(1):119. https://doi.org/10.1186/s13058-020-01350-2
14. Kim HO, Kim JS, Shin YM, Ryu JS, Lee YS, Lee SG. Evaluation of metabolic characteristics and viability of lipiodolized hepatocellular carcinomas using 18F-FDG PET/CT. J Nucl Med. 2010;51(12):1849–56. https://doi.org/10.2967/jnumed.110.079244
15. Lin CY, Chen JH, Liang JA, Lin CC, Jeng LB, Kao CH. 18F-FDG PET or PET/CT for detecting extrahepatic metastases or recurrent hepatocellular carcinoma: a systematic review and meta-analysis. Eur J Radiol. 2012;81(9):2417–22. https://doi.org/10.1016/j.ejrad.2011.08.004
16. Hirmas N, Leyh C, Sraieb M, Barbato F, Schaarschmidt BM, Umutlu L, et al. 68Ga-PSMA-11 PET/CT Improves Tumor Detection and Impacts Management in Patients with Hepatocellular Carcinoma. J Nucl Med. 2021;62(9):1235–1241. https://doi.org/10.2967/jnumed.120.257915
17. Ho CL, Yu SC, Yeung DW. 11C-acetate PET imaging in hepatocellular carcinoma and other liver masses. J Nucl Med. 2003;44(2):213–21.
18. Park JW, Kim JH, Kim SK, Kang KW, Park KW, Choi JI, et al. A prospective evaluation of 18F-FDG and 11C-acetate PET/CT for detection of primary and metastatic hepatocellular carcinoma. J Nucl Med. 2008;49(12):1912–21. https://doi.org/10.2967/jnumed.108.055087
19. Guo W, Pang Y, Yao L, Zhao L, Fan C, Ke J, et al. Imaging fibroblast activation protein in liver cancer: a single-center post hoc retrospective analysis to compare [68Ga]Ga-FAPI-04 PET/CT versus MRI and [18F]-FDG PET/CT. Eur J Nucl Med Mol Imaging. 2021;48(5):1604–1617. https://doi.org/10.1007/s00259-020-05095-0
20. Talbot JN, Fartoux L, Balogova S, Nataf V, Kerrou K, Gutman F, et al. Detection of hepatocellular carcinoma with PET/CT: a prospective comparison of 18F-fluoro choline and 18F-FDG in patients with cirrhosis or chronic liver disease. J Nucl Med. 2010;51(11):1699–706. https://doi.org/10.2967/jnumed.110.075507
21. Fallahi B, Manafi-Farid R, Eftekhari M, Fard-Esfahani A, Emami-Ardekani A, Geramifar P, Akhlaghi M, Hashemi Taheri AP, Beiki D. Diagnostic efficiency of 68Ga-DOTATATE PET/CT as compared to 99mTc-Octreotide SPECT/CT and conventional morphologic modalities in neuroendocrine tumors. Asia Ocean J Nucl Med Biol. 2019 Spring;7(2):129–140. https://doi.org/10.1097/RLU.0000000000003410
22. Johnbeck CB, Knigge U, Loft A, Berthelsen AK, Mortensen J, Oturai P, et al. Head-to-Head Comparison of 64Cu-DOTATATE and 68Ga-DOTATOC PET/CT: A Prospective Study of 59 Patients with Neuroendocrine Tumors. J Nucl Med. 2017;58(3):451–457. https://doi.org/10.2967/jnumed.116.180430
23. Xia Q, Liu J, Wu C, Song S, Tong L, Huang G et al. Prognostic significance of 18FDG PET/CT in colorectal cancer patients with liver metastases: a meta-analysis. Cancer Imaging. 2015;15:19. https://doi.org/10.1186/s40644-015-0055-z
24. Lubezky N, Metser U, Geva R, Nakache R, Shmueli E, Klausner JM, Even-Sapir E, Figer A, Ben-Haim M. The role and limitations of 18-fluoro-2-deoxy-D-glucose positron emission tomography (FDG-PET) scan and computerized tomography (CT) in restaging patients with hepatic colorectal metastases following neoadjuvant chemotherapy: comparison with operative and pathological findings. J Gastrointest Surg. 2007;11(4):472–8. https://doi.org/10.1007/s11605-006-0032-8

25. Kong E, Chun KA, Cho IH. Quantitative assessment of simultaneous F-18 FDG PET/MRI in patients with various types of hepatic tumors: Correlation between glucose metabolism and apparent diffusion coefficient. PLoS One. 2017;12(7):e0180184. https://doi.org/10.1371/journal.pone.0180184
26. Nakanuma Y, Kakuda Y. Pathologic classification of cholangiocarcinoma: New concepts. Best Pract. Res. Clin. Gastroenterol. 2015;29:277–93. https://doi.org/10.1016/j.bpg.2015.02.006
27. Banales JM, Marin JJG, Lamarca A, Rodrigues PM, Khan SA, Roberts LR, et al. Cholangiocarcinoma 2020: the next horizon in mechanisms and management. Nat. Rev. Gastroenterol. Hepatol. 2020 179 2020;17:557–88. https://doi.org/10.1038/s41575-020-0310-z
28. Lamarca A, Barriuso J, Chander A, McNamara MG, Hubner RA, ÓReilly D, et al. 18F-fluorodeoxyglucose positron emission tomography (18FDG-PET) for patients with biliary tract cancer: Systematic review and meta-analysis. J. Hepatol. 2019;71:115–29. https://doi.org/10.1016/j.jhep.2019.01.038
29. Vogel A, Bridgewater J, Edeline J, Kelley RK, Klümpen HJ, Malka D, et al. Biliary tract cancer: ESMO Clinical Practice Guideline for diagnosis, treatment and follow-up 5 behalf of the ESMO Guidelines Committee. Ann. Oncol. 2022;34:127–40. https://doi.org/10.1016/j.annonc.2022.10.506
30. Benson AB, Abrams T, Abbott DE, Ahmed A, Anaya DA, Anders R, et al. Hepatobiliary Cancers, Version 2.2021, NCCN Clinical Practice Guidelines in Oncology. J Natl Compr Canc Netw. 2021 May 1;19(5):541–565.
31. Furlan A, Ferris J V., Hosseinzadeh K, Borhani AA. Gallbladder Carcinoma Update: Multimodality Imaging Evaluation, Staging, and Treatment Options. 2012;191:1440–7. https://doi.org/10.2214/AJR.07.3599
32. Makino I, Yamaguchi T, Sato N, Yasui T, Kita I. Xanthogranulomatous cholecystitis mimicking gallbladder carcinoma with a false-positive result on fluorodeoxyglucose PET. World J. Gastroenterol. 2009;15:3691. https://doi.org/10.3748/wjg.15.3691
33. Maldjian PD, Ghesani N, Ahmed S, Liu Y. Adenomyomatosis of the gallbladder: another cause for a "hot" gallbladder on 18F-FDG PET. AJR Am J Roentgenol. 2007 Jul;189(1):W36–8. https://doi.org/10.2214/AJR.05.1284
34. Majid A, Raju RS, Trochsler M, Kanhere HA, Maddern GJ. Mycobacterial infection of the gallbladder masquerading as gallbladder cancer with a false positive pet scan. Case Rep Med. 2013;2013:828631. https://doi.org/10.1155/2013/828631
35. Tian R, Su M, Tian Y, Li F, Li L, Kuang A, et al. Dual-time point PET/CT with F-18 FDG for the differentiation of malignant and benign bone lesions. Skeletal Radiol. 2009;38:451–8. https://doi.org/10.1007/s00256-008-0643-0
36. Patkar S, Chaturvedi A, Goel M, Rangarajan V, Sharma A, Engineer R. Role of positron emission tomography-contrast enhanced computed tomography in locally advanced gallbladder cancer. J. Hepatobiliary. Pancreat. Sci. 2020;27:164–70. https://doi.org/10.1002/jhbp.712
37. Ramos-Font C, Gõmez-Rio M, Rodríguez-Fernández A, Jiménez-Heffernan A, Sánchez RS, Llamas-Elvira JM. Ability of FDG-PET/CT in the detection of gallbladder cancer. J. Surg. Oncol. 2014;109:218–24. https://doi.org/10.1002/jso.23476
38. Kumar R, Sharma P, Kumari A, Halanaik D, Malhotra A. Role of 18F-FDG PET/CT in detecting recurrent gallbladder carcinoma. Clin. Nucl. Med. 2012;37:431–5. https://doi.org/10.1097/RLU.0b013e31824d24c4
39. Lee JY, Kim HJ, Yim SH, Shin DS, Yu JH, Ju DY, et al. Primary Tumor Maximum Standardized Uptake Value Measured on18 F-Fluorodeoxyglucose Positron Emission Tomography-Computed Tomography Is a Prognostic Value for Survival in Bile Duct and Gallbladder Cancer. Korean J. Gastroenterol. 2013;62:227–33. https://doi.org/10.4166/kjg.2013.62.4.227
40. Jo J, Kwon HW, Park S, Oh DY, Cheon GJ, Bang YJ. Prospective Evaluation of the Clinical Implications of the Tumor Metabolism and Chemotherapy-Related Changes in Advanced Biliary Tract Cancer. J. Nucl. Med. 2017;58:1255–61. https://doi.org/10.2967/jnumed.116.186239
41. Lan L, Zhang S, Xu T, Liu H, Wang W, Feng Y, et al. Prospective Comparison of 68Ga-FAPI versus 18F-FDG PET/CT for Tumor Staging in Biliary Tract Cancers. Radiology 2022;304:648–57. https://doi.org/10.1148/radiol.213118
42. Kim JY, Kim M-H, Lee TY, Hwang CY, Kim JS, Yun S-C, et al. Clinical Role of 18F-FDG PET-CT in Suspected and Potentially Operable Cholangiocarcinoma: A Prospective Study Compared With Conventional Imaging. Off. J. Am. Coll. Gastroenterol. JACG 2008;103. https://doi.org/10.1111/j.1572-0241.2007.01710.x

43. Kendall T, Verheij J, Gaudio E, Evert M, Guido M, Goeppert B, et al. Anatomical, histomorphological and molecular classification of cholangiocarcinoma. Liver Int. 2019;39:7–18. https://doi.org/10.1111/liv.14093
44. Fritscher-Ravens A, Bohuslavizki KH, Broering DC, Jenicke L, Schafer H, Buchert R, et al. FDG PET in the diagnosis of hilar cholangiocarcinoma. Nucl. Med. Commun. 2001;22. https://doi.org/10.1097/00006231-200112000-00002
45. Choi BI, Lee JH, Han MC, Kim SH, Yi JG, Kim CW. Hilar cholangiocarcinoma: comparative study with sonography and CT. 172:689–92. https://doi.org/10.1148/radiology.172.3.2549565
46. Kato T, Tsukamoto E, Kuge Y, Katoh C, Nambu T, Nobuta A, et al. Clinical role of 18F-FDG PET for initial staging of patients with extrahepatic bile duct cancer. Eur. J. Nucl. Med. 2002;29:1047–54. https://doi.org/10.1007/s00259-002-0852-z
47. Pang L, Bo X, Wang J, Wang C, Wang Y, Liu G, et al. Role of dual-time point 18F-FDG PET/CT imaging in the primary diagnosis and staging of hilar cholangiocarcinoma. Abdom. Radiol. 2021;46:4138–47. https://doi.org/10.1007/s00261-021-03071-2
48. Ma KW, Cheung TT, She WH, Chok KSH, Chan ACY, Dai WC, Chiu WH, Lo CM. Diagnostic and Prognostic Role of 18-FDG PET/CT in the Management of Resectable Biliary Tract Cancer. World J Surg. 2018 Mar;42(3):823–834. https://doi.org/10.1007/s00268-017-4192-3
49. Prytz H, Keiding S, Björnsson E, Broomé U, Almer S, Castedal M, Munk OL; Swedish Internal Medicine Liver Club. Dynamic FDG-PET is useful for detection of cholangiocarcinoma in patients with PSC listed for liver transplantation. Hepatology. 2006 Dec;44(6):1572–80. https://doi.org/10.1002/hep.21433
50. Wang J, Shao Y, Liu B, Wang X, Geist BK, Li X, et al. Dynamic 18F-FDG PET imaging of liver lesions: evaluation of a two-tissue compartment model with dual blood input function. BMC Med. Imaging 2021;21:1–13. https://doi.org/10.1186/s12880-021-00623-2
51. Veldhuijzen van Zanten SEM, Pieterman KJ, Wijnhoven BPL, Pruis IJ, Groot Koerkamp B, van Driel LMJW, et al. FAPI PET versus FDG PET, CT or MRI for Staging Pancreatic-, Gastric- and Cholangiocarcinoma: Systematic Review and Head-to-Head Comparisons of Diagnostic Performances. Diagnostics (Basel). 2022 Aug 12;12(8):1958. https://doi.org/10.3390/diagnostics12081958
52. Pang Y, Hao B, Shang Q, Sun L, Chen H. Comparison of 68Ga-FAPI and 18F-FDG PET/CT in a Patient with Cholangiocellular Carcinoma: A Case Report. Clin. Nucl. Med. 2020;45:566–7. https://doi.org/10.1097/RLU.0000000000003056